THERMOCHEMICAL AND KINETIC DATABASES FOR THE SOLAR CELL SILICON MATERIALS

K. Tang[1], E.J. Øvrelid[1], G. Tranell[2], M. Tangstad[2]

[1] SINTEF Materials and Chemistry, N-7465 Trondheim, Norway; kai.tang@sintef.no
[2] Norwegian University of Science and Technology, N-7491 Trondheim, Norway

ABSTRACT

The fabrication of solar cell grade silicon (SOG-Si) feedstock involves processes that require direct contact between solid and a fluid phase at near equilibrium conditions. Knowledge of the phase diagram and thermochemical properties of the Si-based system is important for providing boundary conditions in the analysis of processes. A self-consistent thermodynamic description of the Si-Ag-Al-As-Au-B-Bi-C-Ca-Co-Cr-Cu-Fe-Ga-Ge-In-Li-Mg-Mn-Mo-N-Na-Ni-O-P-Pb-S-Sb-Sn-Te-Ti-V-W-Zn-Zr system has recently been developed by SINTEF Materials and Chemistry. The assessed database has been designed for use within the composition space associated with the SoG-Si materials. Impurity diffusion coefficients for Ag, Al, As, Au, B, Bi, C, Co, Cr, Cu, Fe, Ga, In, Li, Mn, N, Ni, O, P, S, Sb, Te, Ti and Zn in both solid and liquid silicon have been critically reviewed and modelled. The databases can be regarded as the state-of-art relations for the phase equilibria and impurity diffusivities in the Si-based multicomponent system. Examples of applying the databases to evaluate the effect of third element on the carbon solubility and effective segregation coefficient of phosphorus have been demonstrated.

1 INTRODUCTION

The success of producing and refining Si feedstock materials from so-called metallurgical grade to solar cell grade purity depend heavily on the availability and reliability of thermodynamic, kinetic and other physical data for the most common and important SoG-Si trace elements. For example, knowledge of the phase diagram and thermochemical properties of the Si-based system is important for providing boundary conditions in the analysis of processes. However, thermodynamic and kinetic data for these elements in the ppm and ppb ranges are scarce and often unreliable. More importantly, to our knowledge, no dedicated SoG-Si database exists which has gathered and optimized existing data on high purity Si alloys.

In this paper, a self-consistent thermodynamic description of the Si-Ag-Al-As-Au-B-Bi-C-Ca-Co-Cr-Cu-Fe-Ga-Ge-In-Li-Mg-Mn-Mo-N-Na-Ni-O-P-Pb-S-Sb-Sn-Te-Ti-V-W-Zn-Zr system is introduced[1]. The database covers all 34 silicon-impurity binary systems. Among these binary silicon-containing systems, the Si-Al, Si-C, Si-Fe, Si-N, Si-O, Si-P, Si-S, Si-Sb and Si-Te systems have been thermodynamically “re-optimized” based primarily on the assessed experimental information. Since thermodynamic calculations for the impurities in SoG-Si feedstock are normally multi-dimensional in nature, Gibbs energies of 36 other binary systems have also been included in the database. In this way, the effect of other impurities on the phase equilibria of principle impurity in SoG-Si materials can be reliably evaluated. Systematic validation of the database has been carried out using the experimental data for Si-based multicomponent systems, and examples of the validation are given in the following section.

The Czochralski method of growing single crystal silicon is affected by thermocapillary convection[2]. Temperature and concentration gradients at the free surface of the melt give rise to surface tension-driven Marangoni flow, which can lead to crystal defects, if it is sufficiently large. To this end, the assessed thermochemical database has further been extended to calculate the surface tensions of liquid Si-based melts, subject to the constraint of Gibbs energy minimization. In addition to thermodynamic properties, the temperature and composition gradients of surface tension in Si-based melts can be simultaneously calculated using the database. The databases can be regarded as the state-of-art equilibrium relations in the Si-based multicomponent system.

Impurity diffusion coefficients for Ag, Al, As, Au, B, Bi, C, Co, Cr, Cu, Fe, Ga, In, Li, Mn, N, Ni, O, P, S, Sb, Te, Ti and Zn in both solid and liquid silicon have been critically assessed[3]. The self diffusivity of Si in both solid and liquid silicon has also been extensively investigated. Coupling of the critical evaluated diffusivities with the thermochemical description in determination of the effective segregation coefficients were also discussed in the paper.

2 THE ASSESSED THERMOCHEMICAL DATABASE

Aluminum, boron, carbon, iron, nitrogen, oxygen, phosphorus, sulfur and titanium are the common impurities in the SoG-Si feedstock. Arsenic and antimony are frequently used as doping agents. Transition metals (Co, Cu, Cr, Fe, Mn, Mo, Ni, V, W, Zr), alkali and alkali-earth impurities (Li, Mg, Na) as well as Bi, Ga, Ge, In, Pb, Sn, Te and Zn may appear in the SoG-Si feedstock. A thermochemical database that covers these elements has recently been developed at SINTEF Materials and Chemistry, which has been designed for use within the composition space associated with the SoG-Si materials. All the binary and several critical ternary subsystems have been assessed and calculated results have been validated with the reliable experimental data in the literature. The database can be regarded as the state-of-art equilibrium relations in the Si-based multicomponent system.

As illustrated in Figure 1:, the composition space of impurity in the SoG-Si materials generally ranges from ppb to a few percent[1]. The database covers all 33 silicon-impurity binary systems. Among the 33 binary silicon-containing systems, the Si-Al, Si-As, Si-B, Si-C, Si-Fe, Si-N, Si-O, Si-P, Si-S, Si-Sb and Si-Te systems have thermodynamically been “re-optimized” based primarily on the assessed experimental information. Since thermodynamic calculations for the impurities in SoG-Si feedstock are normally multi-dimensional in nature, Gibbs energies of 36 other binary systems have also been included in the database. In this way, the effect of other impurities on the phase equilibria of principle impurity in SoG-Si materials can be reliably evaluated. Systematic validation of the database has been carried out using the experimental data for Si-based multicomponent systems. Examples of the validation will be given in the following section.

2.1 Thermodynamic description

The SGTE formulism[4] has been selected for the representation of the Gibbs energy of the pure elements and the stoichiometric compounds. Compounds with a narrow range of homogeneity, for example SiB_6 and SiB_3, are treated as stoichiometric compounds in the database.

The liquid Si-based solution, here abbreviated as *l*, is described using a simple polynomial expression based on a substitutional solution with random mixing. The same model is employed for the diamond-structured Si-rich solid phase, denoted as *s*. The Gibbs energies of the liquid and solid Si-based phases are given by the following equation:

$$G_m^f = x_{Si}^f \, {}^0G_{Si}^f + \sum_{i \neq Si} x_i^f \, {}^0G_i^f + RT(x_{Si}^f \ln x_{Si}^f + \sum_{i \neq Si} x_i^f \ln x_i^f) + {}^{Ex}G_m^f \quad (f = l, s) \tag{1}$$

where ${}^0G_{Si}^f$ and ${}^0G_i^f$ are, respectively, the molar Gibbs energy of Si and element *i* with the phase ϕ in a nonmagnetic state, The second term is the contribution of ideal mixing. The excess Gibbs energy, ${}^{Ex}G_m^f$, is expressed in the Redlich-Kister polynomial:

$$ {}^{Ex}G_m^f = \sum_i \sum_j x_i^f x_j^f \sum_{k=0}^{n} {}^kL_{ij}^f (x_i^f - x_j^f)^k \tag{2}$$

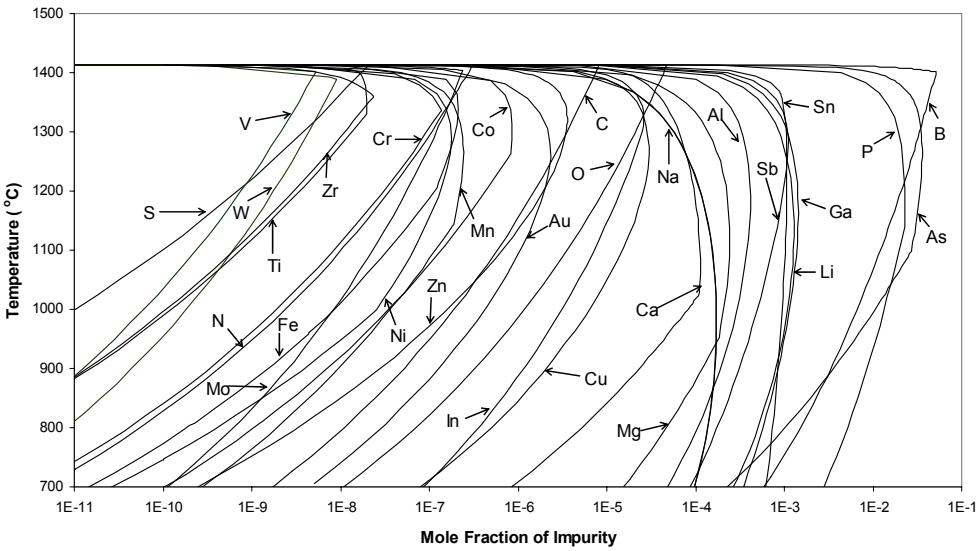

Figure 1: Solubilities of the impurities in solid silicon

Since the concentrations of impurities in solar cell grade silicon are in the range from ppb to a few percent, it is not necessary to take ternary interaction parameters into account. The activity coefficient of impurity, *i*, in a multicomponent system is given by Eq.(3):

$$RT\ln g_i^f = {}^{Ex}G_m^f + \frac{\partial\, {}^{Ex}G_m^f}{\partial x_i^f} - \sum_{j=1}^{n} x_j^f \frac{\partial\, {}^{Ex}G_m^f}{\partial x_j^f} \qquad (3)$$

For SoG-Si materials, $x_i^f \to 0$ and $x_{Si}^f \to 1$, so the Henrian activity coefficient of component *i* can be approximately expressed:

$$g_i^f \approx \exp\left(\sum_{k=0}^{n} {}^{k}L_{Si-i}^f \Big/ RT\right) \quad (f = l,s) \qquad (4)$$

The assessed model parameters, ${}^{k}L_{ij}^f$, for the liquid and solid phases in the Si-rich Si-B-C-Fe system are listed in Table 1. Thermodynamic descriptions of the solid compounds are taken from the SGTE pure substance thermochemical database.

Table 1: Thermodynamic descriptions of the liquid and solid Si-rich Si-B-C-Fe system in SI unit

Liquid phase (J/mol)	Solid phase (J/mol)
${}^{0}L_{SiB}^{Liq} = 17632\text{-}1.7632T$	${}^{0}L_{SiB}^{Sol} = 66884\text{-}17.25T$
${}^{1}L_{SiB}^{Liq} = -\ 3527\text{+}0.353T$	${}^{0}L_{SiC}^{Sol} = 90000\text{+}4.5T$
${}^{0}L_{SiC}^{Liq} = -\ 15700\text{+}6.52T$	${}^{0}L_{SiFe}^{Sol} = 137650\text{-}8.12T$
${}^{0}L_{SiFe}^{Liq} = -\ 164434.6\text{+}41.9773T$	
${}^{1}L_{SiFe}^{Liq} = 0 - 21.523T$	
${}^{2}L_{SiFe}^{Liq} = -\ 18821.5\text{+}22.07T$	
${}^{3}L_{SiFe}^{Liq} = -\ 9695.8$	

2.2 Surface Tension

Following the theoretical treatment given by Guggenheim[5] and Bulter[6], a monolayer surface phase is assumed in equilibrium with the bulk liquid phase. Since the surface tension is the reversible work required to extend a surface by a unit area at constant temperature, pressure and composition, it is necessary to take the area into consideration for the Gibbs energies of the species in the surface phase. A fictitious species, "Area", is thus introduced to the surface phase[7]. The components of surface phase are assumed to be "Area"-related: SiA_m, BA_n, CA_p, OA_q, …*etc*. The stoichiometric coefficients of the "Area"-related components can be determined by the normalized molar surface area of pure element:

$$m = A_i / A_0, \quad n = A_j / A_0, \quad \text{L} \tag{5}$$

where A_i, A_j, … are the molar surface areas of pure elements and A_0 the normalization constant. The numerical value of A_0 is in principle arbitrary. For the best numerical performance of Gibbs energy minimization and for the sake of the common interfacial tension unit (mN/m), a value 1000 is used for A_0 in the present study. The chemical potentials of components in the surface phase are determined by following equation:

$$m_i^S = m_i^0 + RT \ln a_i^S + A_i s_i \tag{6}$$

here σ_i is the surface tension of pure element *i* and μ_i^0 the chemical potential of *i* in the bulk phase.

Elements B, C, N and O are normally either in the form of solid or gas in the temperature range of interest. The molar surface areas and surface tensions of the metastable B, C, N and O liquids have been estimated from the experimental values. The criterion of equilibrium between the bulk and surface phase leads to following equation for component *i*:

$$A_i(s - s_i) = RT(\ln a_i^S - \ln a_i^B) \tag{7}$$

Eq.(7) can be used for the determination of the molar surface area of *i*, if the measured interfacial tension, σ, is available. A special code has been developed for this purpose. At equilibrium, the following simple linear relation holds[8]:

$$G = \sum_l b_l m_l \tag{8}$$

here b_l is the total molar amount of system component *l* in the system. This means that the chemical potential of the fictitious component, μ_{Area}, is equivalent to the surface tension of liquid melt, σ, in the unit of mN/m (because the normalization constant, A_0, is used with the unit m^2/mol). In this way, surface tension of a multicomponent melt can be directly determined by Gibbs energy minimization technique under the following mass and an additional "Area" balance constraints:

$$\sum_i \sum_l \left(a_{il}^B n_i^B + a_{il}^S n_i^S\right) = b_l \tag{9}$$

$$\sum_l (A_l^S / A_0) n_l^S = A / A_0 \tag{10}$$

where a_{il}^B and a_{il}^S are the coefficients of the stoichiometric matrices of components in bulk and surface phases, n_i^B and n_i^S are the molar numbers of species in bulk and surface phases, respectively.

2.3 Equilibrium distribution coefficient

Segregation effects at the liquid-solid interface are controlled by the equilibrium distribution coefficient, k_i^{eq}, which is defined as the ratio of the solidus and the liquidus concentrations in mole fractions. Applying the phase equilibrium rule to this case results in the formula for the determination of equilibrium distribution coefficient:

$$k_i^{eq} = \frac{g_i^l}{g_i^s} \exp\left(\frac{\Delta^0 G_i^{fus}}{RT}\right) \quad (11)$$

here $\Delta^0 G_i^{fus}$ refers the Gibbs energy of fusion of impurity *i* at temperature T. Activity coefficients of impurity *i* in liquid and solid phases can be determined using Eq.(4).

2.4 Typical assessments

The assessment for the Si-C system will briefly be introduced in this section.

The new assessment for the Si-C system was based primarily on experimental SiC solubility data in liquid solution given by Scace and Slack[9], Hall[10], Iguchi[11], Kleykamp and Schumacher[12], Oden and McCune[13] and Ottem[14]. Solid solubility data given by Nozaki *et al*.[15], Bean[16] and Newman[17] were used to determine the properties of solid solution. The eutectic composition reported by Nozaki *et al*.[15] and Hall[10] and peritectic transformation temperature determined by Scace[9] and Kleykamp[12] were also used in the thermodynamic optimization. Thermodynamic description of the SiC compound was taken from an early assessment[18]. The calculated SiC solubilities in liquid and solid Si-C solutions are compared with the experimental values in Figure 2:. Calculated SiC solubilities in liquid silicon have been confirmed by the most recent measurements carried out by Dakaler and Tangstad[19]

The modeled surface tension and its temperature gradient for the Si-O melts at different oxygen partial pressures are shown in Figure 4: and Figure 5:,respectively. Thermodynamic descriptions of the bulk and surface phases in the Si-O system are given in Table 2. The calculation results can reproduce the experimental data[20-24] within their uncertainties.

Table 2: Thermodynamic descriptions of the surface and bulk phases in Si-O system in SI unit

Bulk phase: (Si, O) mixture	Surface phase: ($SiA_{45.8}$-OA_{232}) mixture
m_{Si}^0 from Ref. [4]	$m_{Si}^S = m_{Si}^0$ +58257-11.46T
m_O^0 from Ref. [4]	$m_O^S = m_O^0$+2000-0.2T
${}^0L_{SiO}^{Liq}$ = -303630+50T from Ref. [25]	${}^0L_{SiA_{45.8}-OA_{232.2}}^{Liq}$ = -273267+45T from Ref. [25]

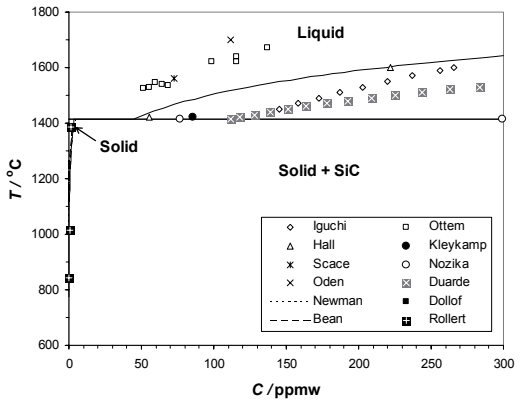

Figure 2: The assessed Si-C system in the Si-rich domain

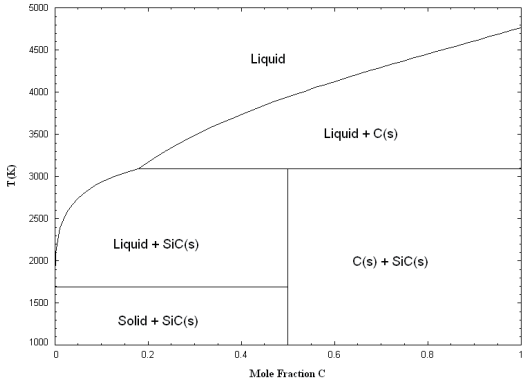

Figure 3: The new assessed Si-C system

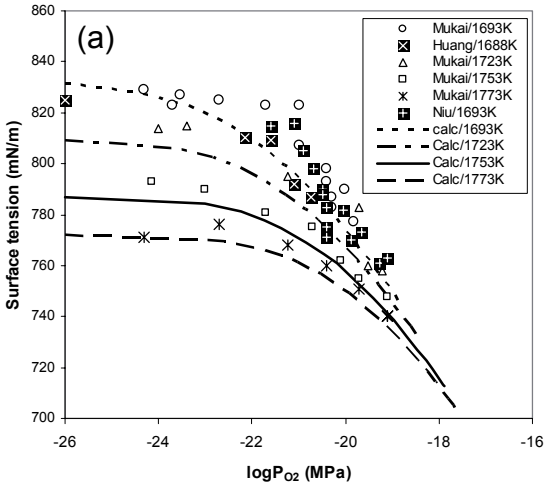

Figure 4: Calculated surface tension of Si-O melt

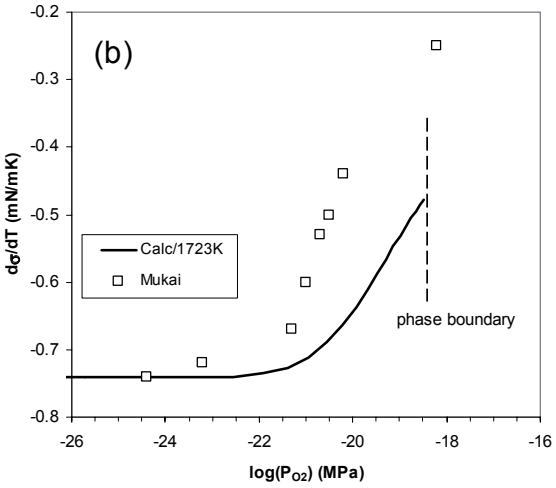

Figure 5: Calculated temperature gradient of surface tension in Si-O melt

3 THE KINETIC DATABASE

3.1 Impurity diffusivity in solid silicon

Mechanisms for the solid diffusions are well-defined[26]. The impurity diffusivity in solid silicon is usually described by the Arrhenius-type equation:

$$D = D_0 \exp(-\frac{E}{kT}) \tag{12}$$

where D_0 is the pre-exponential factor and E is the diffusion activation energy. The parameters D_0 and E can be evaluated from the measurements of diffusion coefficients at a series of temperatures. Since composition space of the common impurities generally ranges from ppb to a few percent, the impurity diffusivity is generally assumed to be composition-independent.

The assessment of the impurity diffusivity is basically similar to those for the thermodynamic properties. Experimental data were first collected from the literature. Each piece of selected experimental information was then given a certain weight factor. The weight factor can in principle be assigned in such a way that those obtained directly from temperature dependence profiles, effects of high concentration and heavy doping measurements are higher than those for the cooperative effects with other dopants. The weight factor could be changed until a satisfactory description of the majority of the selected experimental data was reproduced.

3.2 Impurity diffusivity in liquid silicon

The mechanisms for the liquid diffusion are not well established yet. The Arrhenius equation, Eq.(12), is still the standard description for the liquid impurity diffusivity. The pre-exponential factor and activation energy can be either fitted from the experimental data, or based on the first principle simulation[27-29] and semi-empirical correlations[30, 31], when no experimental value is available.

For those no experimental data available, the impurity diffusivity in liquid silicon can approximately be represented by the self-diffusivity. Several semi-empirical models[30-32] were proposed in the literature. Liu *et al*.[30] proposed a predictive equation to estimate the solute diffusivity in liquid metal based primarily on the work of Cahoon[32]:

$$D_{AB}^{l} = D_0 \frac{d_B}{d_A} \exp(-\frac{0.17 T_m (16 + K_0)}{T}) \tag{13}$$

where d_A and d_B the Goldschmidt diameter of A and B atom, T_m is the melting temperature of solute species. K_0 is the atomic valence; its values are, respectively, 1, 2 and 3 for the bcc, hcp and fcc structure.

Recently, Iida *et al*.[31] proposed a model for the prediction of self-diffusivity of liquid metallic elements based mainly on the modified Stokes-Einstein formula with the authors' early model[33]:

$$D = D_0 \exp(-\frac{16T_m^{1.07}}{RT}) \quad (14)$$

with

$$D_0 = 2.19x10^{-16}\left(\frac{\xi_T T_m}{M}\right)^{0.5}\frac{T_m}{C_0 g_m V_m^{1/3}}\exp\left(\frac{16T_m^{0.07}}{R}\right) \quad (15)$$

where the C_0 is a constant (≈ 0.369 $kg^{-0.5}m^{-1}sK^{0.5}mol^{0.5}$) that is approximately the same for all metals, M is the atomic mass, γ_m is the surface tension, ξ_T is a parameter introduced by the authors, *T* is the absolute temperature and subscript m denotes melting point. These semi-empirical correlations have been used to evaluate the experimental data. For the impurities whose experimental data are not available, the above semi-empirical correlations were used to estimate the liquid impurity diffusivities.

Figure 6: shows the assessed 23 impurity diffusivities in both the solid and liquid silicon in the temperature range of practical interest. Figure 7: is the enlarge portion of Figure 6: for the liquid impurity diffusivities.

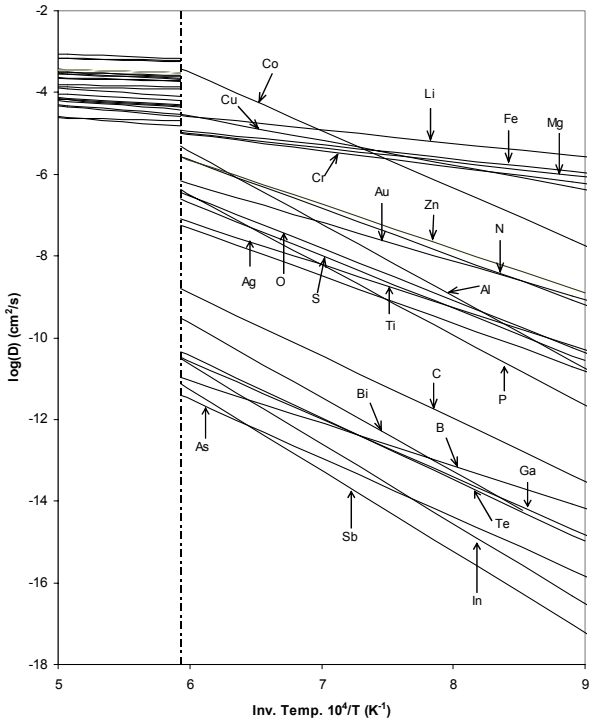

Figure 6: The assessed impurity diffusivities in solid and liquid silicon

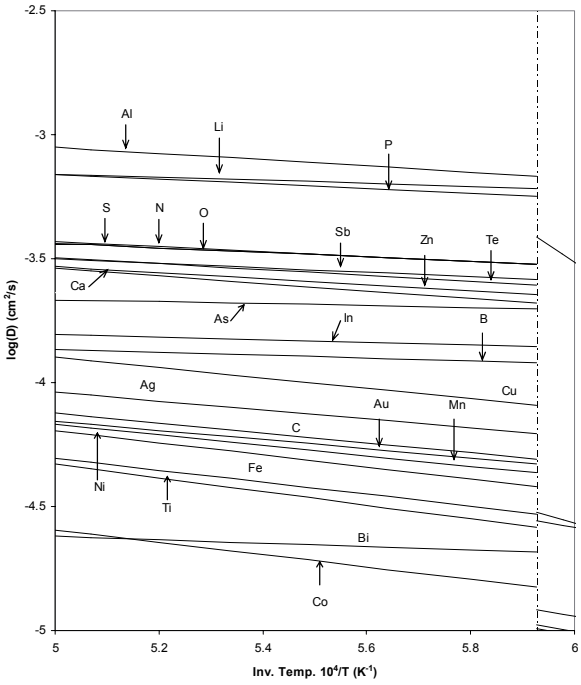

Figure 7: The assessed impurity diffusivities in liquid silicon

3.3 Typical assessments

The assessed impurity diffusivities of C in both the solid and liquid silicon will be briefly introduced in this section. The measured diffusivities in liquid silicon were also identified by the error bar given by the original author(s).

Carbon diffuses in solid silicon both substitutionally and interstitially. It has been experimentally confirmed that carbon diffuses substitutionally in solid silicon at high temperatures[17]. The carbon diffusivities in liquid silicon measured by Pampuch *et al*.[34] were used in the present kinetic database. Figure 8: shows the assessed carbon diffusivity in liquid and solid silicon.

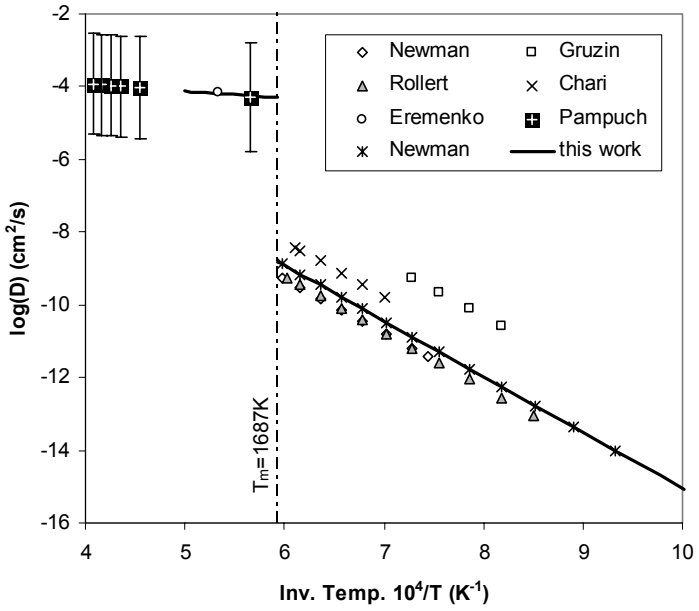

Figure 8: Diffusivity of C in solid and liquid silicon with the experimental data

4 APPLICATION

Applications of the assessed thermochemical and kinetic databases have been extensively studied and shown elsewhere[35]. Only a few examples will be presented in this paper.

4.1 Effect of Third Element on the Carbon Solubility in Liquid Silicon

The assessed thermodynamic properties of liquid and solid Si-based solution can be directly applied to evaluate the influence of third element on the solubility of the main impurity in silicon melt. For example, the effect of the impurity element on the solubility of C in pure Si melt can be evaluated.

Figure 9: shows the evaluated effect of impurities elements on the solubility of carbon in pure Si. Addition of Zr, P, B, Zn, As, Mn and Al leads to increased carbon solubility while addition of O, Cr, Cu, Ca, Fe, Ni, S and N has the opposite influence. Comparing these results with the experimental results reported by Yanaba *et al*[36], the model calculations are satisfactory.

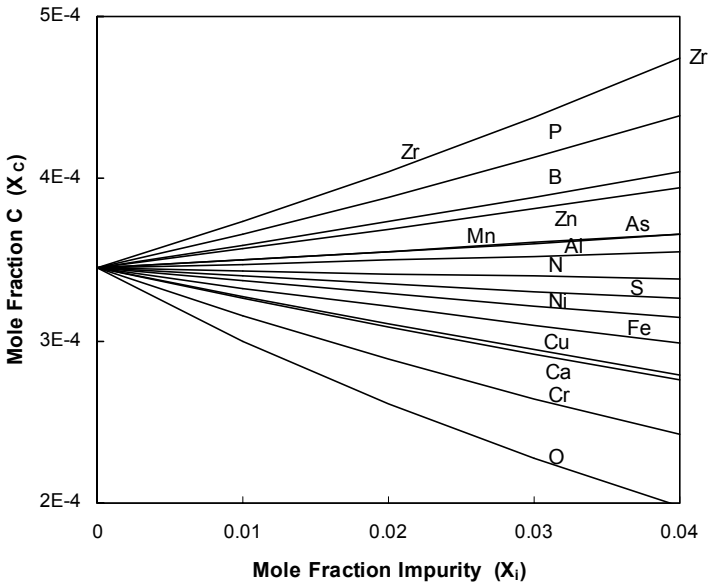

Figure 9: Effect of element on the carbon solubility in liquid silicon at 1500°C

4.2 Effective Segregation Coefficient of Phosphorus

The equilibrium segregation coefficient, k_0, is applicable for solidification only at a negligibly slow growth rate. In the real silicon crystal growth process, with the start of solidification at a given solid-liquid interface, segregation takes place and the rejected impurity atoms begin to accumulate in the melt layer near the growth interface. An impurity concentration gradient thus develops just ahead of the advancing solid crystal.

The effective segregation coefficient, k_{eff}, defined by the Burton-Prim-Slichter equation, Eq.(16), is often used in practice to classify the impurity segregation behaviors in silicon. Taking the thickness of boundary layer δ, the solidification rata ν, and the diffusivity of the impurity D in the liquid phase into account, the effective segregation coefficient can be defined at any moment if stirring and convection currents in the liquid remain virtually uniform[37]:

$$k_{eff} = \frac{k_0}{k_0 + (1 - k_0)\exp(-\frac{vd}{D})} \qquad (16)$$

The silicon rich part of the Si-P phase diagram at high temperatures has recently been re-determined experimentally by Safarian *et al*.[38] The distribution coefficient of P in Si was found to be 0.12, using the determined solidus and liquidus data. These values are significant lower than 0.35, as reported in the literature[39].

Dependence of the phosphorus effective distribution coefficient upon silicon crystal growth rate and rotation rate with three given k_0 values is shown in Figure 10: and Figure 11:,respectively. k_{eff} is largely independent of the rotation rate, when ω is faster than 10 rpm. On the other hand, k_{eff} increases monotonously with increasing crystal growth rate. Assuming the phosphorus equilibrium segregation coefficient is 0.35, k_{eff} is always higher than the general accepted value. On the other hand, k_{eff} can only approach the value 0.35 for k_0=0.15 at very low rotation rate (<5 rpm) and high growth rate (>0.006 cm/s). We then assume that the k_0 is close to 0.25, under the normal crystal growth condition, e.g. ω=10-20 rpm and v=2-4 mm/min, finding k_{eff} is in the range between 0.32 to 0.36. It is thus concluded that the phosphorus equilibrium distribution coefficient is likely to the value around 0.25.

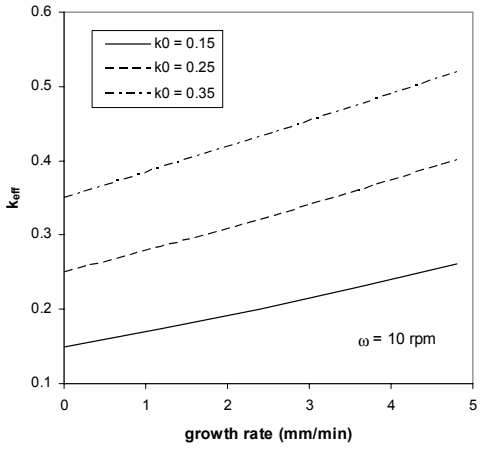

Figure 10: Dependence of phosphorus effective segregation coefficient on the silicon crystal growth rates at temperature near melting point of silicon

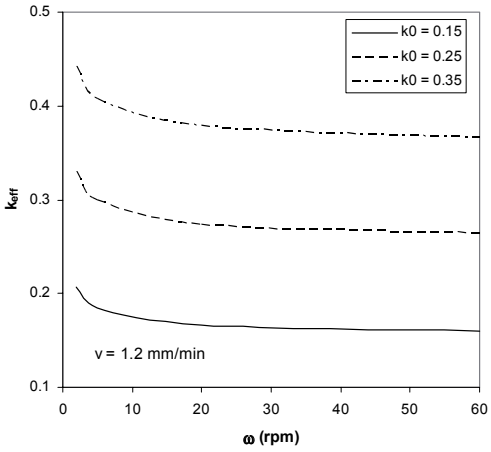

Figure 11: Dependence of phosphorus effective segregation coefficient on the silicon crystal rotation rates at temperature near melting point of silicon

5 CONCLUSIONS

A self-consistent thermochemical description of the Si-Ag-Al-As-Au-B-Bi-C-Ca-Co-Cr-Cu-Fe-Ga-Ge-In-Li-Mg-Mn-Mo-N-Na-Ni-O-P-Pb-S-Sb-Sn-Te-Ti-V-W-Zn-Zr system has recently been developed by SINTEF Materials and Chemistry. The assessed database has been designed for use within the composition space associated with the SoG-Si materials. The thermochemical database has further been extended to simulate the surface tension of liquid Si-based melts. The surface-related properties, *e.g.* temperature and composition gradients, surface excess quantity are able to directly obtain from the database.

The diffusion of impurities in solid and liquid silicon are critically reviewed and assessed in the present paper. The activation energies and pre-exponential factors in the Arrhenius equation have been evaluated using the least-squares analysis and semi-empirical correlations. Impurity diffusion coefficients for Ag, Al, As, Au, B, Bi, C, Co, Cu, Fe, Ga, Ge, In, Li, Mn, Mn, N, Na, Ni, O, P, S, Sb, Sn, Te, Ti and Zn in both solid and liquid silicon have been obtained. The databases can be regarded as the state-of-art equilibrium relations in the Si-based multicomponent system.

Applications of the thermochemical and kinetic databases to determine the effect of third element on the carbon solubility and effective segregation coefficient of phosphorus have been demonstrated in the paper.

6 REFERENCES

[1] Tang, K., Ovrelid, E. J., Tranell, G., and Tangstad, M.: Materials Transactions, **50**(2009)8, pp. 1978-1984.
[2] Mills, K. C. and Courtney, L.: Isij International, **40**(2000)Supplement, pp. S130-S138.
[3] Tang, K., Øvrelid, E., Tranell, G., and Tangstad, M.: JOM, **61**(2009)11, pp. 49-55.
[4] Dinsdale, A. T.: Calphad, **15**(1991)4, pp. 317-425.
[5] Guggenheim, E. A. : Transactions of the Faraday Society, **41**(1945) pp. 150-156.
[6] Bulter, J.A.V.: Proceedings of the Royal Sociaty, **A135**(1932) pp. 348-375.
[7] Pajarre, R., Koukkari, P., Tanaka, T., and Lee, J.: Calphad, **30**(2006)2, pp. 196-200.
[8] Eriksson, G. and Hack, K.: Metallurgical Transactions B-Process Metallurgy, **21**(1990)6, pp. 1013-1023.
[9] Scace, R. I. and Slack, G. A.: The Journal of Chemical Physics, **30**(1959)6, pp. 1551-1555.
[10] Hall, R. N.: Journal of applied physics, **29**(1958)6, pp. 914-917.

[11] Iguchi, Y. and Narushima, T. *First International Conference on Processing Materials for Properties*. 1991
[12] Kleykamp, H. and Schumacher, G.: Berichte der Bunsen-Gesellschaft-Physical Chemistry Chemical Physics, **97**(1993)6, pp. 799-805.
[13] Oden, L. L. and Mccune, R. A.: Metallurgical Transactions A-Physical Metallurgy and Materials Science, **18**(1987)12, pp. 2005-2014.
[14] Ottem, L., *L›selighet og termodynamiske data for oksygen og karbon i flytende legeringer av silisium og ferrosilisium*. 1993, SINTEF Metallurgy: Trondheim, Norway. pp. 1-124.
[15] Nozaki, T., Yatsurugi, Y., and Akiyama, N.: Journal of the Electrochemical Society, **117**(1970) pp. 1566-1568.
[16] Bean, A. R. and Newman, R. C.: Journal of Physics and Chemistry of Solids, **32**(1971)6, pp. 1211-1219.
[17] Newman, R. C.: Materials Science and Engineering B, **36**(1996)1-3, pp. 1-12.
[18] Grobner, J., Lukas, H. L., and Anglezio, J. C.: Calphad-Computer Coupling of Phase Diagrams and Thermochemistry, **20**(1996)2, pp. 247-254.
[19] Dalaker, H. and Tangstad, M., *Time and temperature dependence of the solubility of carbon in liquid silicon*, in *the 23rd European Photovoltaic Solar Energy Conference*. 2008: Valencia, Spain.
[20] Lukin, S. V., Zhuchkov, V. I., and Vatolin, N. A.: Journal of the Less Common Metals, **67**(1979)2, pp. 399-405.
[21] Mukai, K., Yuan, Z., Nogi, K., and Hibiya, T.: Isij International, **40**(2000)Supplement, pp. S148-S152.
[22] Mukai, K. and Yuan, Z. F.: Materials Transactions Jim, **41**(2000)2, pp. 331-337.
[23] Huang, Xinming, Togawa, Shinji, Chung, Sang-Ik, Terashima, Kazutaka, and Kimura, Shigeyuki: Journal of Crystal Growth, **156**(1995)1-2, pp. 52-58.
[24] Niu, Z., Mukai, K., Yutaka, S, Shiraishi, Y., Hibiya, T., Kakimoto, K. , and Koyama, M. : Journal of the Japanese Association of Crystal Growth, **23**(1996)5, pp. 374-381.
[25] Schnurre, S. M., Grobner, J., and Schmid-Fetzer, R.: Journal of Non-Crystalline Solids, **336**(2004)1, pp. 1-25.
[26] Beke, D. L., Allen, C. E., Bracht, H., Bruff, C. M. , Dutt, M. B. , Erdelyi, G. , Gas, P., D'heurle, F. M. , Murch, G E., Seebauer, E G., Sharma, B. L. , and Stolwijk, N. A., *Diffusion in Semiconductors*. 1998, Beke, D. L.: Springer
[27] Stich, I., Car, R., and Parrinello, M.: Physical Review B, **44**(1991)9, pp. 4262-4274.
[28] Wang, C. Z., Chan, C. T., and Ho, K. M.: Physical Review B, **45**(1992)21, pp. 12227.
[29] Yu, W., Wang, Z. Q., and Stroud, D.: Physical Review B, **54**(1996)19, pp. 13946.
[30] Liu, Y., Long, Z., Wang, H., Du, Y., and Huang, B.: Scripta Materialia, **55**(2006)4, pp. 367-370.
[31] Iida, Takamichi, Guthrie, Roderick, and Tripathi, Nagendra: Metallurgical and Materials Transactions B, **37**(2006)4, pp. 559-564.
[32] Cahoon, J.: Metallurgical and Materials Transactions A, **28**(1997)3, pp. 583-593.
[33] Iida, T and Guthrie, R.I.L., *The Physical Properties of Liquid Metals*. 1993: Oxford University Press, Oxford, U.K.
[34] Pampuch, R., Walasek, E., and Bialoskórski, J.: Ceramics International, **12**(1986)2, pp. 99-106.
[35] Tang, K., Ovrelid, E. J, Tranell, G., and Tangstad, M., *Thermochemical and Kinetic Databases for the Solar Cell Silicon Materials, in Crystal Growth of Silicon for Solar Cells*. 2009: Spinger
[36] Yanaba, K., Matsumura, Y., Narushima, T., and Iguchi, Y.: Materials Transactions Jim, **39**(1998)8, pp. 819-823.
[37] Burton, J. A., Prim, R. C., and Slichter, W. P.: The Journal of Chemical Physics, **21**(1953)11, pp. 1987-1991.
[38] Safarian , J., Tangstad , M., and Gaal, S., *Thermal Analysis of Silicon-Phosphorus Alloys at Elevated Temperatures*, in *3rd International Workshop on Crystalline Silicon Solar Cells*, L. Arnberg, Editor. 2009: Trondheim, Norway.
[39] Trumbore, F. A.: The Bell System technical journal : a journal devoted to the scientific and engineering aspects of electrical communication, **39**(1960) pp. 205-233.